Soft Matter

PAPER

View Article Online
View Journal | View Issue

Cite this: *Soft Matter*, 2021, **17**, 1692

Globular protein assembly and network formation at fluid interfaces: effect of oil†

Jotam Bergfreund, *[a] Michael Diener, [a] Thomas Geue, [b] Natalie Nussbaum, [a] Nico Kummer, [ac] Pascal Bertsch, [a] Gustav Nyström [ac] and Peter Fischer *[a]

Received 20th October 2020,
Accepted 13th December 2020

DOI: 10.1039/d0sm01870h

rsc.li/soft-matter-journal

The formation of viscoelastic networks at fluid interfaces by globular proteins is essential in many industries, scientific disciplines, and biological processes. However, the effect of the oil phase on the structural transitions of proteins, network formation, and layer strength at fluid interfaces has received little attention. Herein, we present a comprehensive study on the effect of oil polarity on globular protein networks. The formation dynamics and mechanical properties of the interfacial networks of three different globular proteins (lysozyme, β-lactoglobulin, and bovine serum albumin) were studied with interfacial shear and dilatational rheometry. Furthermore, the degree of protein unfolding at the interfaces was evaluated by subsequent injection of disulfide bonds reducing dithiothreitol. Finally, we measured the interfacial layer thickness and protein immersion into the oil phase with neutron reflectometry. We found that oil polarity significantly affects the network formation, the degree of interfacial protein unfolding, interfacial protein location, and the resulting network strength. These results allow predicting emulsion stabilization of proteins, tailoring interfacial layers with desired mechanical properties, and retaining the protein structure and functionality upon adsorption.

Introduction

Proteins are amphiphilic biomacromolecules, known to adsorb to fluid–fluid interfaces. Protein adsorption leads to a decrease in interfacial energy, rearrangement of the protein conformation, and assembly into viscoelastic 2D nanofilms.[1–3] These processes are of interest in various scientific disciplines and industries. In particular, emulsion stabilization by proteins is crucial in food production, pharmaceutical formulations, agrochemical commodities, and in encapsulation processes.[3–7] Furthermore, proteins stabilize vital foams and emulsions utilized as endogenous biotic materials by animals[8,9] and the viscoelastic protein layers serve as substrates for stem cell proliferation and for bacterial biofilms.[10–13] Moreover, protein behavior at fluid interfaces gains attention in nutritional, medical, and pharmaceutical research in areas such as protein crystallization, lipid bodies, protein digestion, antibody stability, vaccination efficiency, biomimicking protocells, and cell membrane functions.[14–19]

Protein adsorption is governed by the physicochemical properties of both subphases. Previous research focused almost exclusively on the role of temperature, concentration, and precondition of proteins, as well as the parameters in the aqueous phase, including pH and ionic strength.[2,20–24] The impact of the chemical properties of the hydrophobic subphase is widely neglected and systematic studies are missing, even though a small number of publications indicated changes in interfacial processes at different hydrophobic interfaces.[23,25–30]

Globular proteins, such as β-lactoglobulin (BLG), bovine serum albumin (BSA), and hen egg white lysozyme (LSZ), consist of an amino acid chain which arranges into well-defined secondary and tertiary structures. In water, they have a sphere-like native configuration with most of their hydrophilic amino acid groups at the exterior and hydrophobic residues located at the interior. The native structure is considerably stabilized by hydrophobic interactions and disulfide bonds between cysteine residues.[3] The number and in particular the position of the cysteine residues which form disulfide bonds determine the protein stability. LSZ has distant cysteine groups forming disulfide bonds ensuring a more stable structure. However, BSA's cysteine group is located closely on the primary structure, resulting solely in a local stabilization. BLG has the lowest structural stability, due to a small number of cysteine residues.[31]

[a] *Institute of Food, Nutrition and Health, ETH Zürich, 8092 Zürich, Switzerland. E-mail: jotam.bergfreund@hest.ethz.ch, peter.fischer@hest.ethz.ch; Tel: +41 (0)44 632 53 49*
[b] *Laboratory of Neutron Scattering and Imaging, Paul Scherrer Institut, 5232 Villigen PSI, Switzerland*
[c] *Laboratory for Cellulose & Wood Materials, Swiss Federal Laboratories for Materials Science and Technology (Empa), Dübendorf, 8600, Switzerland*

† Electronic supplementary information (ESI) available. See DOI: 10.1039/d0sm01870h

Most globular proteins adsorb at fluid interfaces in a distinct orientation, with their hydrophobic cavity towards apolar oil phases. However, molecular dynamics simulations predict that at interfaces of oils with increased polarity, proteins adsorb randomly oriented and increasingly insert themselves into the hydrophobic phase.[32] Proteins encounter stronger interfacial elongational stresses at interfaces with lower polarity, which accelerate unfolding.[33] Analysis of the protein configuration in solution and after interfacial adsorption resulted in an increased rearrangement of the secondary and tertiary structures at less at polar oil interfaces.[31,34,35] Therefore, it is expected that protein adsorption and unfolding are governed by oil polarity. The pure oil–water interfacial tension γ_0 is regarded a good measure for oil polarity.[36] The rearrangement of the tertiary structure at fluid interfaces can be amplified by addition of disulfide-bond reducing agents such as dithiothreitol (DTT).[37]

In earlier studies, we elucidated the role of oil chemistry on the adsorption of charged anisotropic cellulose nanocrystals and various proteins. A clear correlation between the oil polarity and the adsorption behavior was found.[28,38] Furthermore, it was shown that the oil properties significantly control the interfacial network rheology and formation kinetics of BLG.[29] Herein, we systematically investigate the influence of oil polarity on layer formation and rheological strength of the 2D nanolayers of three different well-studied globular proteins (BLG, BSA, and LSZ) at fluid interfaces. Additionally, neutron reflectometry was applied to elucidate the interfacial layer structure depending on subphase polarity. In order to highlight the fundamental differences in interfacial behavior, low protein concentrations and long adsorption time-scales were chosen. *n*-Octane, 1-chlorooctane, and 1-octanol were selected as their hydrophobic structure consists of an identical aliphatic 8-carbon chain with an increasingly more polar head group, to ensure a high comparability.

Experimental section

Materials

BLG (97%) was provided by the Food and Bioprocess Engineering group at the Technical University of Munich.[39] LSZ (>95%) was purchased by VWR, and BSA (>98%) by Sigma-Aldrich. The proteins were dissolved in a pH 7 phosphate buffer (10 mM; Milli-Q-water; $Na_2HPO_4{\cdot}H_2O$, Acros Organics; $NaH_2PO_4{\cdot}2H_2O$, Sigma-Aldrich). *n*-Hexane (Merck), *n*-octane (Acros), 1-chlorooctane (Alfa Aesar), MCT (BASF), octanal (Acros), 1-octanol (Sigma Aldrich), and methyl-tert butyl ether (Sigma Aldrich) were purified from polar contaminants with magnesium silicate Florisil ($MgO{\cdot}SiO_2$, 100–200 mesh, Sigma-Aldrich) as described in the literature.[40] The purity was tested with a droplet profile tensiometer, to ensure the correct and constant interfacial tension to pure buffer. Solutions of 20 mM dithiothreitol (DTT, Merck) were dissolved in 10 mM phosphate buffer at pH 7.

Methods

Interfacial shear rheology. The viscoelastic shear properties of the protein adsorption layer were measured with a shear rheometer (MCR 501, Anton Paar) equipped with a biconical disk geometry, as described by Erni *et al.*[41] The network formation at a pure oil–water interface was initiated by injecting 50 mL of 1 g L^{-1} protein solution to the aqueous phase while simultaneously extracting the same volume from the aqueous bulk, to ensure a constant interface height. This method is described in detail in an earlier work.[29] The final protein bulk concentration was 0.243 ± 0.006 g L^{-1} in the interfacial measurement, determined by measuring the extracted protein concentration with a total organic carbon analyzer (TOC-L, Shimadzu). The interfacial time sweep was performed at a deformation of 0.3% and a frequency of 1 rad s^{-1}. After reaching equilibrium, an amplitude sweep was performed from 0.1–100% at 1 rad s^{-1}, to verify that the measurement was performed in the linear viscoelastic regime. A general overview on interfacial rheology is given by Sagis,[42] Erni,[43] as well as Fuller and Vermant.[44]

Dilatational rheology. The purity of the oil phase was confirmed by measuring the constant oil–water interfacial tension with a droplet profile tensiometer (PAT-1, SINTERFACE Technologies), as described in the literature.[28,29,38,45,46] An oil droplet was formed at the tip of an U-shaped capillary tip in 10 mg L^{-1} protein solution. The interfacial tension was extracted from the contour of the drop, monitored using a charge-coupled device camera, by axisymmetric drop shape analysis. For dilatational rheology experiments, the drop was kept at a constant surface area for 12 h to ensure complete protein adsorption and an equilibrated interfacial layer. The linear viscoelastic regime was confirmed with an amplitude sweep from 0.5 to 2%. Each oscillation cycle was performed for 30 min with a constant frequency of $\omega = 0.01$ s^{-1}. Between each oscillation cycle, the drop was kept at a constant surface area for 20 min to ensure an equilibrated drop. Dilatational modulus E' was extracted from the data according to Rühs *et al.*[46,47] at the area change $\delta A/A_0 = 2\%$.

DTT injection to interfacial shear rheology. For the DTT injection experiments, 20 mL of 20 mM DTT in 10 mM pH 7 phosphate buffer solution were injected with simultaneous extraction of 20 mL bulk solution. The approximated DTT concentration in the measurement system was 2 mM. This results in a DTT concentration in the two orders of magnitude higher than the number of cysteine. The circular dichroism spectroscopy (JASCO, EastonMD) spectra showed only slight changes in the protein structure after 24 h in solution upon addition of 5 mM DTT in bulk (see the ESI,† Fig. S1). The DTT injection was started once the protein interfaces reached steady G' and G'' values. The time sweep experiment was continued until the system equilibrated again, followed by an amplitude sweep to validate the viscoelastic linearity.

Neutron reflectivity. Interfacial neutron reflectivity experiments were performed at SINQ, the Swiss Spallation Neutron Source at Paul Scherrer Institute (Villigen PSI, Switzerland) with an AMOR time-of-flight reflectometer.[48] A custom-made aluminium Langmuir trough was used. Experiments were performed with 65 mL of 0.01 wt% and 0.1 wt% BLG at 25 °C. The protein solution was covered with methyl *tert*-butyl ether (MTBE) or *n*-hexane. The reflectivity measurement was started after 3 h, when the oil phase was macroscopically evaporated and a constant interface, D_2O phosphate buffer covered with a thin layer of oil, was formed.

Neutron reflection was recorded at three angles of incidence θ (0.5, 1.3, and 2.8°) and varying neutron wavelengths λ (3.5 to 12 Å), thereby covering a q range of 0.01–0.187 Å^{-1} within 10.5 h at full neutron flux. The first angle of incidence (θ = 0.5°) was repeated at the end of the experiment to verify that the layers did not undergo significant changes. The measured neutron reflectivity was fitted by the Parratt algorithm[49] to assess the interfacial structure of the BLG layers.

Results and discussion

Interfacial shear viscoelasticity of protein layers

The network formation kinetics were observed by measuring the interfacial shear viscoelasticity during the adsorption, rearrangement and interconnection of the proteins at oil–water interfaces (Fig. 1). Initially, the clean oil–water interface with no detectable viscoelastic response is measured. After 5 min, the protein solution is injected at the bottom of the aqueous subphase over a time period of 50 min, as described in an earlier study.[29] Subsequently, the proteins diffuse to the interface and adsorb gradually. After a certain time which is specific for respective combinations of oil and protein, the interfacial storage modulus G' increases. At this point, a continuous detectable interface has developed. In the following time, G' increases and crosses the interfacial shear loss modulus G'' at the cross-over time, indicated with red circles in Fig. 1. At the cross-over time a sufficient number of proteins cover the interface to form a covalently bond network or a jammed network with dominant elastic properties. Finally, G' and G'' asymptotically equilibrate toward the final values, G'_∞ and G''_∞. Amplitude sweeps were measured after equilibration to ensure that the measurements were performed in the linear regime, shown in the ESI† (Fig. S2). We monitored the interfacial network formation of the globular proteins BLG, BSA, and LSZ at the *n*-octane, 1-chlorooctane, and 1-octanol interfaces. Increasing oil polarity in Fig. 1 is represented from dark to light colors and indicated with red arrows. The cross-over time is delayed with an increase in oil polarity for all proteins. This delay arises from slower adsorption kinetics and stronger competition between the proteins and the polar oil molecules at the interface.[29,38]

The viscoelastic response upon shear stresses is weaker for BSA layers at all oils (Fig. 1a) compared to BLG layers (Fig. 1b), which is in good agreement with the literature.[22] Nevertheless, both, BSA and BLG interfaces, are developing lower G'_∞ at more polar oils, due to the decreased unfolding and the plasticizing effect of the incorporated polar oils in the network. The fast network formation indicates an unfolded and interconnected network for BLG and BSA at apolar interfaces. At polar interfaces, BLG and BSA only partly unfolded and incorporated oil molecules interfere with protein–protein interactions and weaken the network. At the 1-octanol interfaces, the BSA network is weakened to an extent that no viscoelastic response was detected over a measuring time of 100 h. LSZ network formation differs significantly (Fig. 1c). LSZ forms interfaces with identical G'_∞ at all subphases. Furthermore, the onset, the cross-over time, and the equilibrated G'_∞ are reached after significantly longer times compared to fast unfolding BLG and BSA. Mitropoulos *et al.*[22] also found that LSZ layers have longer network formation times compared to BSA and BLG and G'_∞ are independent of the hydrophobic subphase, measured for air–water and limonene–water interfaces. LSZ has the most compact structure and the highest unfolding energy of the three proteins.[22] Simulations showed no preferred spatial adsorption orientation and no significant difference in the protein–octane interaction energy between the compact and extended states.[50] Structural analysis indicated no consequential changes in its tertiary structure of adsorbed LSZ. In particular, the disulfide bonds remain intact.[31,51–54] Hence, LSZ adsorbs in its native structure with minor structural changes and forms non-covalent aggregated networks at fluid interfaces.[55] The formation of a continuous interfacial layer with native LSZ requires more time. Thus, we suggest that due to the absence of significant structural expansion an increased number of adsorbed proteins form a jammed network. Furthermore, the higher amount of LSZ at the interfaces leads to a denser interface with a comparably high G'_∞. In conclusion, the interfacial network formation dynamics of globular proteins are governed by the adsorption driving forces

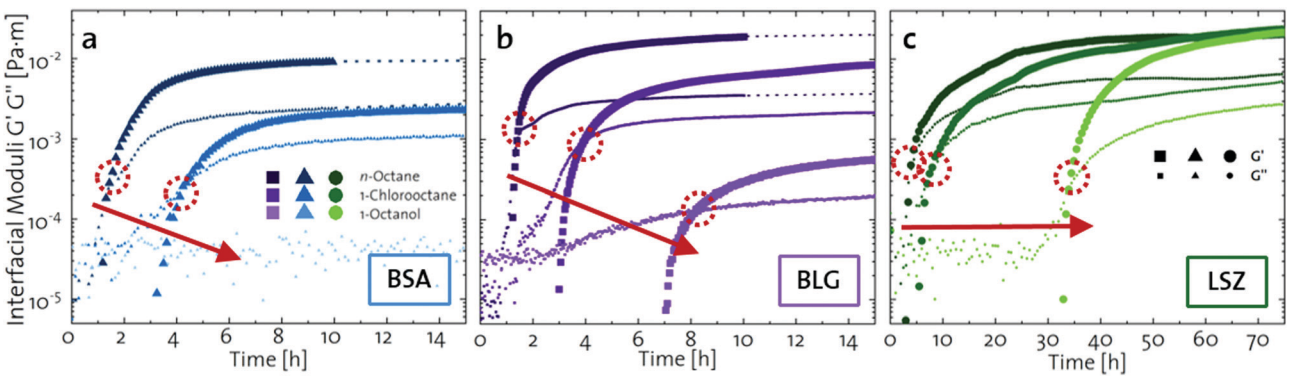

Fig. 1 Interfacial shear time sweeps of the network formation of (a) BSA, (b) BLG, and (c) LSZ at the *n*-octane, 1-chlorooctane, and 1-octanol interfaces. Red circles indicate the cross-over time and the red arrows indicate the increase in oil polarity. Data for BLG are taken from an earlier publication.[29] The equilibrated moduli of BLG and BSA at *n*-octane after 10 h are extrapolated with dotted lines.

at the different interfaces as well as the protein interfacial location, unfolding, and intermolecular interactions, which all change with oil property.

Dilatational rheology of interfacial protein layers

The viscoelastic response of the adsorbed protein layer at oil droplet interfaces upon expansion and compression, the dilatational moduli, was measured after the protein interfaces reached a steady state (constant interfacial pressure). The adsorption kinetics of proteins at these interfaces were reported in a previous contribution.[38] All interfacial layers displayed a pronounced elastic response ($E' > E''$). The dilatational elastic moduli E' are demonstrated in Fig. 2 as a function of γ_{ow}. Additionally, E' values from the literature were incorporated,[27,29,56–62] listed in the ESI† (Table S1). All the experimental data from the literature were measured within pH 6.7–7.0, an ionic strength of 10–150 mM and a protein concentration higher than the minimal interfacial coverage, above which a constant equilibrated interfacial pressure is measured (0.005–0.007 for BSA,[63,64] 0.002 for BLG,[62,65] and 0.001–0.002 for LSZ[64,66]). At apolar interfaces the network exhibited the highest mechanical strength, which decreases with more polar oils. The dilatational viscoelastic moduli of globular protein at oil interfaces can be generalized (black dotted fit in Fig. 2) by:

$$E' \propto 0.5 \cdot \gamma_{ow}^{4/3} \quad (1)$$

The dependency of the network formation of globular proteins on oil–water surface tension derives from two mechanisms: (a) polar interfaces have lower surface stresses,[33] which leads to slower and less protein unfolding. Furthermore, polar oils interact increasingly by hydrogen bonds with the hydrophilic residues at the exterior of the native proteins. This decreases the thermodynamic driving force to rearrange the hydrophobic residues towards the oil phase.[29,32] The decreased rearrangement of the protein secondary and tertiary structure at more polar interfaces was confirmed with structural analysis and simulations.[31,34,35]

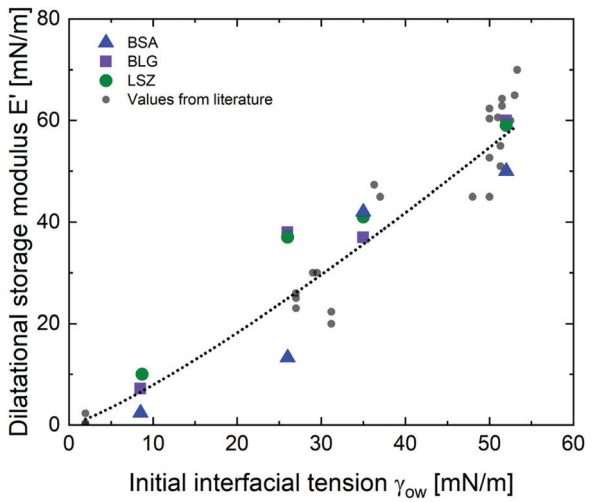

Fig. 2 Elastic dilatational modulus E' of BSA, BLG, and LSZ plotted over γ_{ow}. The black dotted line represents the fit for all globular proteins (eqn (1)) including values from the literature,[27,29,56–62] listed in the ESI† (Table S1).

(b) Molecules of the polar oils are incorporated into the protein network leading to softening of the mechanical properties. The increased polar interaction of the hydrophilic protein residues and the polar oils enable the oils to act as plasticizers and reduce the interconnectivity of the protein layers. At more polar interfaces, the proteins are conserved in a more native structure and the formation of intermolecular bonds is prevented. These results are in line with earlier findings for BLG,[29] where they were schematically illustrated. Hence, this indicates that the correlation between the interfacial strength and the oil polarity are applicable for other globular proteins.

Protein conformation and DDT-induced unfolding at the oil–water interface

Upon adsorption, globular proteins are presumed to unfold and interconnect at fluid interfaces. However, the adsorption experiments in Fig. 1 indicate that different network structures occur. In particular the difference between fast unfolding (BLG and BSA) and more stable globular proteins (LSZ) is striking. To elucidate the structural conformation of the proteins at the interface, interfacial shear rheology with *in situ* injection of a disulfide bond reducing agent was performed with BLG and LSZ. First, the proteins were injected at the oil–water interfaces. DTT injection was started once an equilibrated network developed, indicated with red arrows in Fig. 3. The time sweep was continued until an equilibrated interface was reached. The amplitude sweeps of the equilibrated DTT-reduced interfacial networks confirmed that the measurements were performed in the linear regime and that the rupture of the interfacial networks follow a gel-like behavior, shown in the ESI† (Fig. S3). CD measurements were performed to follow the denaturation of the proteins in the bulk phase upon the addition of DTT. The conformational changes are negligible in bulk after 24 h, shown in the ESI† (Fig. S1). However, DTT is a slightly interfacial active compound, as shown in the ESI† (Fig. S4) and in the literature.[67] Due to the increased interfacial DTT concentration, the protein unfolding is increased by disulfide bond reduction at fluid interfaces. Furthermore, the constant or increasing G' and G'' moduli after DTT injection in Fig. 3 show that DTT does not displace the proteins at the interfaces, as reported for highly surface active surfactants.[68] At the start of the DTT injection, G' and G'' drop slightly due to mechanic destabilization of the interface through the injection process itself. The injection pump system induced a flow in the aqueous phase which results in an intermediate weakening of the network.

The BLG network at the apolar *n*-octane interface in Fig. 3a remains unaffected by the DTT injection. This is in line with neutron reflectometry measurements at the air–water interface, which showed no effect on the BLG layer thickness after addition of 20 mM DTT.[37] At polar interfaces, an increase of G' and G'' was detected following a lag phase. The long lag phases originate from the low electrostatic attraction between the negatively charged deprotonated thiolate of DTT and the negative charged BLG at pH7. The gain in G' and G'' and the lag phase were more pronounced at the most polar 1-octanol

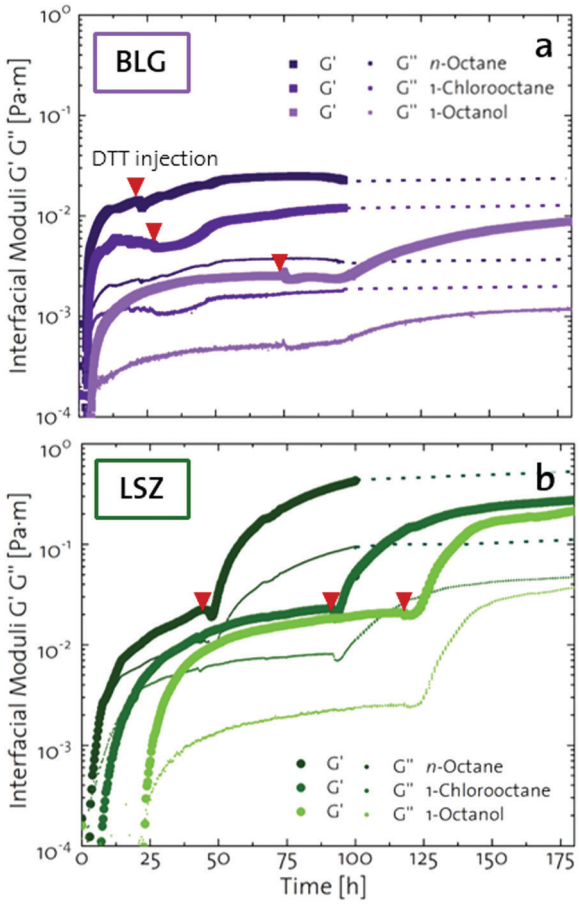

Fig. 3 Interfacial shear rheology time sweeps of (a) BLG and (b) LSZ at oil interfaces with different polarities with a subsequent injection of the disulfide bond reducing agent DTT. The red arrows indicate the point of DTT injection. The dotted lines indicate the extrapolation of equilibrated moduli.

interfaces. The unaffected G'_∞ underlines that all BLG molecules are unfolded at the apolar *n*-octane. Furthermore, the absence of layer weakening evidences that BLG layers are not cross-linked by intermolecular disulfide bonds as proposed in the literature,[30,69] but rather connected by intermolecular β-sheets.[70] In 1-chlorooctane, BLG is partly conserved in a more native structure. The native molecules are then unfolded by the injected DTT, resulting in a G' increase. The same behavior is found more pronounced at 1-octanol, as more BLG is in their native configuration. The final viscoelastic modulus after DTT injection is still dependent on the oil polarity, even though all proteins are unfolded. These differences originate from the plasticizing effect of the incorporated polar oils.

Fig. 3b shows that G' and G'' of LSZ networks increase considerably by up to the order of one magnitude at all interfaces with a distinctly shorter lag phase than BLG after DTT injection. The reduced lag phase arises due to electrostatic attraction between the negatively charged deprotonated thiolate of DTT and the positively charged LSZ at pH 7. The disulfide bond reduction leads to a rearrangement of LSZ at the interface into a significantly more elastic layer. This confirms literature findings, which showed interfacial LSZ unfolding upon disulfide bond reducing agent resulted in a decrease of the surface tension within minutes.[71] Li *et al.* reported that LSZ undergoes a rapid amyloid-like (β-sheet stacking) assembly after unlocking the disulfide bonds by a reducing agent.[71] This further supports that pristine LSZ forms interfacial networks with a mostly native protein conformation. The equilibrated viscoelastic moduli after DTT injection revealed a dependency on the oil polarity, in more polar oils lower G'_∞ and G''_∞ are gained. Therefore, LSZ is also affected by the plasticizing incorporation of polar oils after LSZ loses its native configuration. These results emphasize that more stable proteins (LSZ) form an interfacial network best described by a 2D particle gel and fast unfolding proteins (BLG and BSA) form 2D cross-linked polymer gels.

Structure of the adsorbed interfacial layer

Elucidating the morphology of interfacial networks at oil–water interfaces is challenging, as the covering oil phase makes most interfacial characterization techniques difficult to apply. Several attempts were carried out with neutron reflectometry at oil–water interfaces.[72,73] We present a new approach, exploiting the formation of a protein layer at a volatile oil–water interface. Methyl *tert*-butyl ether (MTBE) was used as a polar and *n*-hexane as an apolar oil. Neutron reflectometry was started after 3 h, when a BLG layer was formed and the oil phase was mostly evaporated. Fig. 4a depicts the neutron reflectivity curves of 0.001 g L^{-1} and 0.01 g L^{-1} BLG at air, *n*-hexane, and MTBE interfaces. The reflectivity data were fitted using the Parratt algorithm to obtain structural information of the BLG layers (Fig. 4a). The interfacial layers were best described by a model accounting for a thin covering oil phase, a protein monolayer, and the underlying aqueous phase. The model parameters used for the fit are presented in Fig. 4b in the form of scattering length density profiles as a function of layer depth. The layer thickness and roughness obtained from the fits are compiled in Table 1. In Fig. 4c these results are schematically illustrated. At all interfaces, the layer thickness was independent of the protein concentration, indicating that at the tested concentration BLG forms continuous monolayers. The BLG layer at the air–water interface had a thickness of approximately 14 Å. In bulk, BLG appears at pH 7 mostly as a dimer of two impinging BLG spheres with 35 Å diameter. The dimers are assumed to dissociate upon contact with the interfaces.[37,74] Therefore, BLG rearranges at the air–water interface, resulting in a flattened structure, in agreement with the literature, in which the layers range from 10–21 Å at pH 7.[7,37,75–79] At the apolar *n*-hexane interface, BLG forms interfacial layers of 16 Å thickness. This indicated a similar structure to that at the air–water interface. However, the slightly higher roughness reveals that the hydrophobic parts of BLG are partly dissolved in the hydrophobic subphase, in line with results of Campana *et al.*[73] for BSA at the hexadecane–water interface. A similar layer thickness at apolar and air interfaces was also found for BSA.[73,80] At the polar MTBE–water interfaces, a layer thickness of 32 Å was measured, which shows that BLG remains mostly in its native configuration. Furthermore, the roughness of 20–25 Å

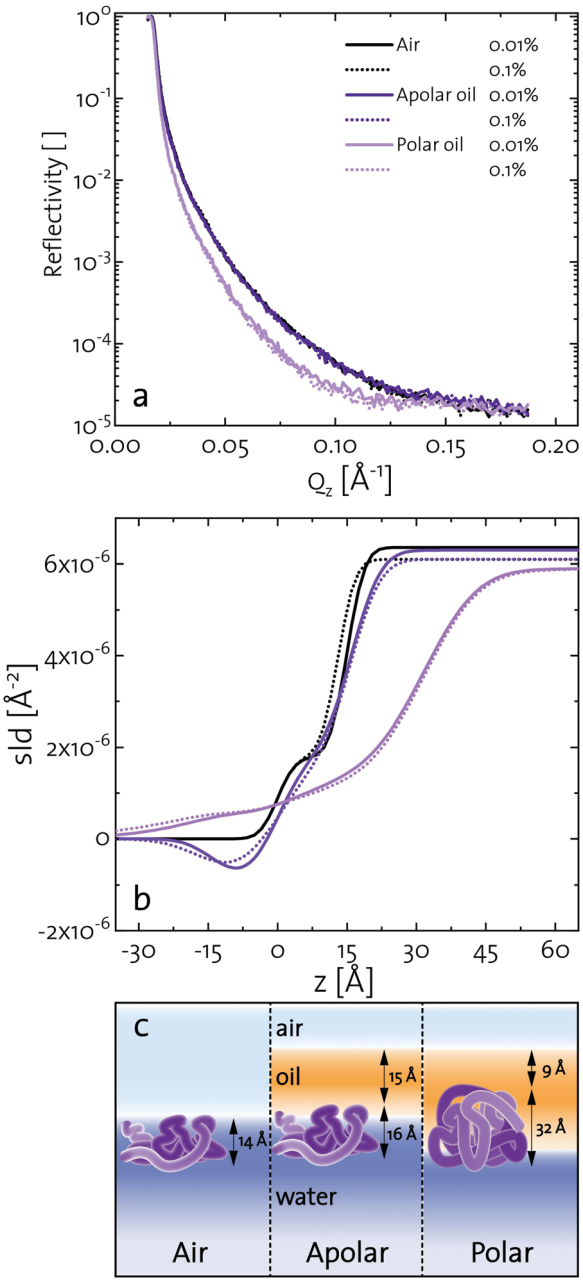

Fig. 4 (a) Neutron reflectivity of BLG layers at air, apolar (*n*-hexane), and polar (MTBE) interfaces for 0.01 and 0.1 wt% BLG concentration. (b) Fitted scattering length densities as a function of layer depth *z*. (c) Schematic illustration of the conformation and location of BLG at different interfaces.

indicates that BLG inserts itself partly into the polar subphase and polar oil molecules are incorporated into the protein network, as predicted in the literature.[29,32] Similar results were found by Jia *et al.*[81] for BSA with dynamic force microscopy. At an apolar interface BSA formed a 30 Å layer and at a polar interface the layer was 60 Å, measured. These results further highlight that fast unfolding proteins such as BLG and BSA rearrange at apolar interfaces. At polar interfaces, these proteins are conserved in their native structure and oil molecules are incorporated into their interfacial layer.

Table 1 Thickness h and roughness σ of BLG layers at air, apolar (*n*-hexane), and polar (MTBE) interfaces obtained from neutron reflectometry and data fitted with the Parratt algorithm

Subphase			Air		*n*-Hexane		MTBE	
BLG	c	[wt%]	0.01	0.1	0.01	0.1	0.01	0.1
Protein layer	h	[Å]	15	13	16	16	32	32
	σ	[Å]	4	4	5	7	20	25
Oil layer	h	[Å]	0	0	14	16	8	10
	σ	[Å]	0	0	5	7	5	5
	χ^2	[10^{-1}]	1.66	1.30	0.34	0.78	2.8	1.04

Conclusions

We have presented a systematic investigation of 2D protein layer assembly at fluid interfaces as a function of protein stability and oil polarity. The interfacial network formation is strongly controlled by the oil polarity. The interfacial viscoelastic strength of the formed protein network is significantly lowered at increasing oil polarity in shear and dilatational rheology. Interfacial shear rheometry reveals that with increasing oil polarity globular proteins require more time to form elastic interfaces. Furthermore, fast unfolding globular proteins such as BLG and BSA form weaker interfacial networks at more polar interfaces. However, LSZ, a more stable globular protein, needs significantly longer network formation times and the final moduli at all interfaces are identical. The dilatational moduli of globular protein layers follow a generalized power law depending on the interfacial tensions of the clean oil–water interfaces and also describe experimental data from previous studies. The protein structural stability upon adsorption to different fluid interfaces was elucidated by performing interfacial shear rheometry with a subsequent injection of disulfide bond reducing DTT. Fast unfolding globular proteins unfold at apolar interfaces and form polymer-like 2D networks and thus remained unaffected by DTT. At interfaces with increased polarity, DTT injection leads to a strengthening of protein layers, indicating that at polar oils the native protein structure is conserved. This is supported by neutron reflectometry measurements, which showed that BLG size is lower at air and apolar oils compared to the bulk. However, at the polar interface, a layer thickness was assessed which corresponds closely to the diameter of a native BLG monomer. The interfacial shear moduli of more stable globular proteins increase drastically upon DTT injection at all interfaces and exhibit a dependency on the oil polarity. Thus, more stable globular proteins remain in their native structure independent of the interface. The gradual decrease in G'_∞ after unfolding at polar interfaces of all proteins originates from the plasticizing incorporation of polar oils into the protein network, resulting in a softening of the interfacial layer. The incorporation of polar oil molecules arises due to their chemical ability to interact with the hydrophilic protein residues.

Our data underline the importance of the oil properties in interfacial protein assembly and its related applications. By choosing a suitable oil, an interfacial protein network with desired viscoelastic properties and protein denaturation state can be achieved. Furthermore, protein adsorption to a polar oil interface may be applied for concentrating protein solution without changing the structural conformation. While this study

broadens the understanding of protein adsorption and network formation at fluid interfaces, there is still a long way ahead of us to be able to fully predict and understand these processes, which are of essential importance in many industries and scientific fields.

Conflicts of interest

There are no conflicts to declare.

Acknowledgements

The authors gratefully acknowledge support from the Swiss National Science Foundation (Grant #: 200021-175994). This work is based on experiments performed at the Swiss Spallation neutron source SINQ, Paul Scherrer Institut, Villigen, Switzerland.

References

1 E. Dickinson, Adsorbed protein layers at fluid interfaces: Interactions, structure and surface rheology, *Colloids Surf., B*, 1999, **15**, 161–176.
2 P. Erni, E. J. Windhab and P. Fischer, Emulsion drops with complex interfaces: Globular versus flexible proteins, *Macromol. Mater. Eng.*, 2011, **296**, 249–262.
3 R. Mezzenga and P. Fischer, The self-assembly, aggregation and phase transitions of food protein systems in one, two and three dimensions, *Rep. Prog. Phys.*, 2013, **76**, 46601.
4 R. Mezzenga, P. Schurtenberger, A. Burbidge and M. Michel, Understanding foods as soft materials, *Nat. Mater.*, 2005, **4**, 729–740.
5 L. Böcker, P. Bertsch, D. Wenner, S. Teixeira, J. Bergfreund, S. Eder, P. Fischer and A. Mathys, Effect of Arthrospira platensis microalgae protein purification on emulsification mechanism and efficiency, *J. Colloid Interface Sci.*, 2021, **584**, 344–353.
6 E. Chantelau and M. Berger, Pollution of insulin with silicone oil, a hazard of disposable plastic syringes, *Lancet*, 1985, **325**, 1459.
7 N. Scheuble, M. Lussi, T. Geue, F. Carrière and P. Fischer, Blocking gastric lipase adsorption and displacement processes with viscoelastic biopolymer adsorption layers, *Biomacromolecules*, 2016, **17**, 3328–3337.
8 A. Cooper, M. W. Kennedy, R. I. Fleming, E. H. Wilson, H. Videler, D. L. Wokosin, T.-J. Su, R. J. Green and J. R. Lu, Adsorption of Frog Foam Nest Proteins at the Air-Water Interface, *Biophys. J.*, 2005, **88**, 2114–2125.
9 P. A. Rühs, J. Bergfreund, P. Bertsch, S. Gstöhl and P. Fischer, 2020, Complex fluids in the animal kingdom, arXiv preprint arXiv:2005.00773.
10 X. Jia, K. Minami, K. Uto, A. C. Chang, J. P. Hill, J. Nakanishi and K. Ariga, Adaptive Liquid Interfacially Assembled Protein Nanosheets for Guiding Mesenchymal Stem Cell Fate, *Adv. Mater.*, 2020, **32**, 1905942.
11 C. Keese and I. Giaever, Cell growth on liquid microcarriers, *Science*, 1983, **219**, 1448–1449.
12 D. Kong, L. Peng, S. Di Cio, P. Novak and J. E. Gautrot, Stem Cell Expansion and Fate Decision on Liquid Substrates Are Regulated by Self-Assembled Nanosheets, *ACS Nano*, 2018, **12**, 9206–9213.
13 P. Rühs, L. Böcker, R. Inglis and P. Fischer, Studying bacterial hydrophobicity and biofilm formation at liquid–liquid interfaces through interfacial rheology and pendant drop tensiometry, *Colloids Surf., B*, 2014, **117**, 174–184.
14 C. N. Nanev, E. Saridakis, L. Govada, S. C. Kassen, H. V. Solomon and N. E. Chayen, Hydrophobic interface-assisted protein crystallization: Theory and experiment, *ACS Appl. Mater. Interfaces*, 2019, **11**, 12931–12940.
15 C. V. Nikiforidis, A. Matsakidou and V. Kiosseoglou, Composition, properties and potential food applications of natural emulsions and cream materials based on oil bodies, *RSC Adv.*, 2014, **4**, 25067–25078.
16 A. Mackie and A. Macierzanka, Colloidal aspects of protein digestion, *Curr. Opin. Colloid Interface Sci.*, 2010, **15**, 102–108.
17 R. Thirumangalathu, S. Krishnan, M. S. Ricci, D. N. Brems, T. W. Randolph and J. F. Carpenter, Silicone oil- and agitation-induced aggregation of a monoclonal antibody in aqueous solution, *J. Pharm. Sci.*, 2009, **98**, 3167–3181.
18 X. Huang, M. Li, D. C. Green, D. S. Williams, A. J. Patil and S. Mann, Interfacial assembly of protein–polymer nanoconjugates into stimulus-responsive biomimetic protocells, *Nat. Commun.*, 2013, **4**, 2239.
19 K. G. Nicholson, A. E. Colegate, A. Podda, I. Stephenson, J. Wood, E. Ypma and M. C. Zambon, Safety and antigenicity of non-adjuvanted and MF59-adjuvanted influenza A/Duck/Singapore/97 (H5N3) vaccine: a randomised trial of two potential vaccines against H5N1 influenza, *Lancet*, 2001, **357**, 1937–1943.
20 P. A. Rühs, N. Scheuble, E. J. Windhab, R. Mezzenga and P. Fischer, Simultaneous control of pH and ionic strength during interfacial rheology of β-lactoglobulin fibrils adsorbed at liquid/liquid interfaces, *Langmuir*, 2012, **28**, 12536–12543.
21 J. Benjamins, J. Lyklema and E. H. Lucassen-Reynders, Compression/expansion rheology of oil/water interfaces with adsorbed proteins. Comparison with the air/water surface, *Langmuir*, 2006, **22**, 6181–6188.
22 V. Mitropoulos, A. Mütze and P. Fischer, Mechanical properties of protein adsorption layers at the air/water and oil/water interface: A comparison in light of the thermodynamical stability of proteins, *Adv. Colloid Interface Sci.*, 2014, **206**, 195–206.
23 S. Roth, B. S. Murray and E. Dickinson, Interfacial shear rheology of aged and heattreated beta-lactoglobulin films: Displacement by nonionic surfactant, *J. Agric. Food Chem.*, 2000, **48**, 1491–1497.
24 E. Dickinson, Proteins at interfaces and in emulsions stability, rheology and interactions, *J. Chem. Soc., Faraday Trans.*, 1998, **94**, 1657–1669.

25 L. Peltonen, J. Hirvonen and J. Yliruusi, The behavior of sorbitan surfactants at the water-oil interface: Straight-chained hydrocarbons from pentane to dodecane as an oil phase, *J. Colloid Interface Sci.*, 2001, **240**, 272–276.
26 E. H. Lucassen-Reynders, J. Benjamins and V. B. Fainerman, Dilational rheology of protein films adsorbed at fluid interfaces, *Curr. Opin. Colloid Interface Sci.*, 2010, **15**, 264–270.
27 J. Maldonado-Valderrama, R. Miller, V. B. Fainerman, P. J. Wilde and V. J. Morris, Effect of gastric conditions on β-lactoglobulin interfacial networks: Influence of the oil phase on protein structure, *Langmuir*, 2010, **26**, 15901–15908.
28 J. Bergfreund, Q. Sun, P. Fischer and P. Bertsch, Adsorption of charged anisotropic nanoparticles at oil–water interfaces, *Nanoscale Adv.*, 2019, **1**, 4308–4312.
29 J. Bergfreund, P. Bertsch, S. Kuster and P. Fischer, Effect of oil hydrophobicity on the adsorption and rheology of β-lactoglobulin at oil–water interfaces, *Langmuir*, 2018, **34**, 4929–4936.
30 D. B. Allan, D. M. Firester, V. P. Allard, D. H. Reich, K. J. Stebe and R. L. Leheny, Linear and nonlinear microrheology of lysozyme layers forming at the air–water interface, *Soft Matter*, 2014, **10**, 7051–7060.
31 L. Day, J. Zhai, M. Xu, N. C. Jones, S. V. Hoffmann and T. J. Wooster, Conformational changes of globular proteins adsorbed at oil-in-water emulsion interfaces examined by synchrotron radiation circular dichroism, *Food Hydrocolloids*, 2014, **34**, 78–87.
32 D. Zare, J. R. Allison and K. M. McGrath, Molecular dynamics simulation of β-lactoglobulin at different oil/water interfaces, *Biomacromolecules*, 2016, **17**, 1572–1581.
33 R. W. Style, L. Isa and E. R. Dufresne, Adsorption of soft particles at fluid interfaces, *Soft Matter*, 2015, **11**, 1–8.
34 J. Zhai, L. Day, M. I. Aguilar and T. J. Wooster, Protein folding at emulsion oil/water interfaces, *Curr. Opin. Colloid Interface Sci.*, 2013, **18**, 257–271.
35 J. Zhai, T. J. Wooster, S. V. Hoffmann, T. H. Lee, M. A. Augustin and M. I. Aguilar, Structural rearrangement of β-lactoglobulin at different oil-water interfaces and its effect on emulsion stability, *Langmuir*, 2011, **27**, 9227–9236.
36 M. El-Mahrab-Robert, V. Rosilio, M. A. Bolzinger, P. Chaminade and J. L. Grossiord, Assessment of oil polarity: Comparison of evaluation methods, *Int. J. Pharm.*, 2008, **348**, 89–94.
37 A. W. Perriman, M. J. Henderson, S. A. Holt and J. W. White, Effect of the air–water interface on the stability of β-Lactoglobulin, *J. Phys. Chem. B*, 2007, **111**, 13527–13537.
38 J. Bergfreund, P. Bertsch and P. Fischer, Adsorption of proteins to fluid interfaces: Role of the hydrophobic subphase, *J. Colloid Interface Sci.*, 2021, **584**, 411–417.
39 J. Toro-Sierra, A. Tolkach and U. Kulozik, Fractionation of α-lactalbumin and β-lactoglobulin from whey protein isolate using selective thermal aggregation, an optimized membrane separation procedure and resolubilization techniques at pilot plant scale, *Food Bioprocess Technol.*, 2013, **6**, 1032–1043.
40 K. Mishra, J. Bergfreund, P. Bertsch, P. Fischer and E. J. Windhab, Crystallization induced network formation of tri-and monopalmitin at the MCT oil/air interface, *Langmuir*, 2020, **26**, 7566–7572.
41 P. Erni, P. Fischer, E. J. Windhab, V. Kusnezov, H. Stettin and J. Läuger, Stressand strain-controlled measurements of interfacial shear viscosity and viscoelasticity at liquid/liquid and gas/liquid interfaces, *Rev. Sci. Instrum.*, 2003, **74**, 4916–4924.
42 L. M. Sagis, Dynamic properties of interfaces in soft matter: Experiments and theory, *Rev. Mod. Phys.*, 2011, **83**, 1367.
43 P. Erni, Deformation modes of complex fluid interfaces, *Soft Matter*, 2011, **7**, 7586–7600.
44 G. G. Fuller and J. Vermant, Complex fluid–fluid interfaces: rheology and structure, *Annu. Rev. Chem. Biomol. Eng.*, 2012, **3**, 519–543.
45 G. Loglio, P. Pandolfini, R. Miller, A. V. Makievski, F. Ravera, M. Ferrari and L. Liggieri, Drop and bubble shape analysis as a tool for dilational rheological studies of interfacial layers, *Stud. Interface Sci.*, 2001, **11**, 439–483.
46 P. A. Rühs, C. Affolter, E. J. Windhab and P. Fischer, Shear and dilatational linear and nonlinear subphase controlled interfacial rheology of β-lactoglobulin fibrils and their derivatives, *J. Rheol.*, 2013, **57**, 1003–1022.
47 P. A. Rühs, N. Scheuble, E. J. Windhab and P. Fischer, Protein adsorption and interfacial rheology interfering in dilatational experiment, *Eur. Phys. J.: Spec. Top.*, 2013, **222**, 47–60.
48 D. Clemens, P. Gross, P. Keller, N. Schlumpf and M. Könnecke, AMOR–the versatile reflectometer at SINQ, *Phys. B*, 2000, **276**, 140–141.
49 L. G. Parratt, Surface studies of solids by total reflection of X-rays, *Phys. Rev.*, 1954, **95**, 359.
50 D. L. Cheung, Adsorption and conformations of lysozyme and α-lactalbumin at a wateroctane interface, *J. Chem. Phys.*, 2017, **147**, 195101.
51 J. R. Lu, T. J. Su, R. K. Thomas, J. Penfold and J. Webster, Structural conformation of lysozyme layers at the air/water interface studied by neutron reflection, *J. Chem. Soc., Faraday Trans.*, 1998, **94**, 3279–3287.
52 C. Postel, O. Abillon and B. Desbat, Structure and denaturation of adsorbed lysozyme at the air–water interface, *J. Colloid Interface Sci.*, 2003, **266**, 74–81.
53 V. Lechevalier, T. Croguennec, S. Pezennec, C. Guérin-Dubiard, M. Pasco and F. Nau, Ovalbumin, ovotransferrin, lysozyme: three model proteins for structural modifications at the air- water interface, *J. Agric. Food Chem.*, 2003, **51**, 6354–6361.
54 M. D. Lad, F. Birembaut, J. M. Matthew, R. A. Frazier and R. J. Green, The adsorbed conformation of globular proteins at the air/water interface, *Phys. Chem. Chem. Phys.*, 2006, **8**, 2179.
55 M. van de Weert, J. Hoechstetter, W. E. Hennink and D. J. Crommelin, The effect of a water/organic solvent interface on the structural stability of lysozyme, *J. Controlled Release*, 2000, **68**, 351–359.
56 E. M. Freer, K. S. Yim, G. G. Fuller and C. J. Radke, Interfacial rheology of globular and flexible proteins at the

hexadecane/water interface: Comparison of shear and dilatation deformation, *J. Phys. Chem. B*, 2004, **108**, 3835–3844.
57 J. Benjamins, A. Cagna and E. Lucassen-Reynders, Viscoelastic properties of triacylglycerol/water interfaces covered by proteins, *Colloids Surf., A*, 1996, **114**, 245–254.
58 J. Benjamins, *Static and dynamic properties of proteins adsorbed at liquid interfaces*, PhD thesis, Wageningen UR, 2000.
59 A. Williams and A. Prins, Comparison of the dilational behaviour of adsorbed milk proteins at the air–water and oil–water interfaces, *Colloids Surf., A*, 1996, **114**, 267–275.
60 É. Kiss and R. Borbás, Protein adsorption at liquid/liquid interface with low interfacial tension, *Colloids Surf., B*, 2003, **31**, 169–176.
61 R. Wüstneck, B. Moser and G. Muschiolik, Interfacial dilational behaviour of adsorbed β-lactoglobulin layers at the different fluid interfaces, *Colloids Surf., B*, 1999, **15**, 263–273.
62 J. Won, G. Gochev, V. Ulaganathan, J. Krägel, E. Aksenenko, V. Fainerman and R. Miller, Dilational visco-elasticity of BLG adsorption layers at the solution/tetradecane interface – Effect of pH and ionic strength, *Colloids Surf., A*, 2017, **521**, 204–210.
63 D. Graham and M. Phillips, Proteins at liquid interfaces, *J. Colloid Interface Sci.*, 1979, **70**, 415–426.
64 A. Berthold, H. Schubert, N. Brandes, L. Kroh and R. Miller, Behaviour of BSA and of BSA-derivatives at the air/water interface, *Colloids Surf., A*, 2007, **301**, 16–22.
65 G. Gochev, I. Retzlaff, E. Aksenenko, V. Fainerman and R. Miller, Adsorption isotherm and equation of state for β-Lactoglobulin layers at the air/water surface, *Colloids Surf., A*, 2013, **422**, 33–38.
66 O. Sudah, G. Chen and Y. Chiew, Adsorption of single component and binary mixtures of protein and surfactants at the oil–water interface, *Colloids Surf., B*, 1999, **13**, 195–202.
67 C. Beverung, C. J. Radke and H. W. Blanch, Protein adsorption at the oil/water interface: characterization of adsorption kinetics by dynamic interfacial tension measurements, *Biophys. Chem.*, 1999, **81**, 59–80.
68 J.-L. Courthaudon, E. Dickinson, Y. Matsumura and D. C. Clark, Competitive adsorption of β-lactoglobulin + Tween 20 at the oil–water interface, *Colloids Surf.*, 1991, **56**, 293–300.
69 E. Dickinson and Y. Matsumura, Time-dependent polymerization of β-lactoglobulin through disulphide bonds at the oil-water interface in emulsions, *Int. J. Biol. Macromol.*, 1991, **13**, 26–30.
70 H. Schestkowa, S. Drusch and A. M. Wagemans, FTIR analysis of β-lactoglobulin at the oil/water-interface, *Food Chem.*, 2020, **302**, 125349.
71 C. Li, L. Xu, Y. Y. Zuo and P. Yang, Tuning protein assembly pathways through superfast amyloid-like aggregation, *Biomater. Sci.*, 2018, **6**, 836–841.
72 L. Lee, D. Langevin and B. Farnoux, Neutron reflectivity of an oil–water interface, *Phys. Rev. Lett.*, 1991, **67**, 2678.
73 M. Campana, S. Hosking, J. Petkov, I. Tucker, J. Webster, A. Zarbakhsh and J. Lu, Adsorption of bovine serum albumin (BSA) at the oil/water interface: a neutron reflection study, *Langmuir*, 2015, **31**, 5614–5622.
74 A. R. Mackie, F. A. Husband, C. Holt and P. J. Wilde, Adsorption of β-Lactoglobulin variants A and B to the air–water interface, *Int. J. Food Sci. Technol.*, 1999, **34**, 509–516.
75 G. G. Gochev, E. Scoppola, R. A. Campbell, B. A. Noskov, R. Miller and E. Schneck, β-Lactoglobulin Adsorption Layers at the Water/Air Surface: 3. Neutron Reflectometry Study on the Effect of pH, *J. Phys. Chem. B*, 2019, **123**, 10877–10889.
76 P. J. Atkinson, E. Dickinson, D. S. Horne and R. M. Richardson, Neutron reflectivity of adsorbed β-casein and β-lactoglobulin at the air/water interface, *J. Chem. Soc., Faraday Trans.*, 1995, **91**, 2847–2854.
77 I. M. Tucker, J. T. Petkov, J. Penfold, R. K. Thomas, A. R. Cox and N. Hedges, Adsorption of hydrophobin–protein mixtures at the air–water interface: the impact of ph and electrolyte, *Langmuir*, 2015, **31**, 10008–10016.
78 N. Scheuble, T. Geue, E. J. Windhab and P. Fischer, Tailored interfacial rheology for gastric stable adsorption layers, *Biomacromolecules*, 2014, **15**, 3139–3145.
79 P. Bertsch, A. Thoma, J. Bergfreund, T. Geue and P. Fischer, Transient measurement and structure analysis of protein–polysaccharide multilayers at fluid interfaces, *Soft Matter*, 2019, **15**, 6362–6368.
80 J. Lu, T. Su and R. Thomas, Structural conformation of bovine serum albumin layers at the air–water interface studied by neutron reflection, *J. Colloid Interface Sci.*, 1999, **213**, 426–437.
81 X. Jia, K. Minami, K. Uto, A. C. Chang, J. P. Hill, T. Ueki, J. Nakanishi and K. Ariga, Modulation of Mesenchymal Stem Cells Mechanosensing at Fluid Interfaces by Tailored Self-Assembled Protein Monolayers, *Small*, 2019, **15**, 1804640.

